Tuijin Jishu/Journal of Propulsion Technology
ISSN: 1001-4055
Vol. 47 No. 02 (2026)

Influence of Welding Current on Nugget Formation and Mechanical Performance of Dissimilar Steel Joints: A Multiphysics Approach

Pratik V. Handge[1], R. M. Choudhari[2], P. V. Chopde[3], Dr. Y. A. Kharche[4], N. A. Kharche[5], S. R. Shekokar[6]

[1]*Research Scholar, Padm. Dr. V. B. Kolte College of Engineering, Malkapur, India*

[2,3,5,6] *Assistant Professor, Padm. Dr. V. B. Kolte College of Engineering, Malkapur, India*

[4] *Associate Professor, Padm. Dr. V. B. Kolte College of Engineering, Malkapur, India*

Abstract: - The current requirement of lightweight and crash-resistant automotive construction methods and the application of multi-material groupings have promoted the extensive application of this material groupings making solid joining of different grades of steel desired. The proposed research investigates the Resistance Spot Welding (RSW) of three dissimilar mixtures: Mild Steel (MS) to Stainless Steel (SS), SS to HSLA 355 Steel (HSLA 355 metal), MS to HSLA 355 metal. The following sequential electro-thermal-mechanical numerical model was established using ANSYS 19.2 to predict nugget assembly and stress distribution. A wide-field experiment which was evaluated was conducted in the welding range 8–12 kA with a constant sheet thickness of 3 mm. Results illustrate an interplay of performance, where the SS-HSS joint displayed the best maximum Tensile Shear Strength at 11 kA of 9.85 kN with the highest TSS: 18.6% enhancement over MS-SS from a baseline standard. The numerical model presented was shown very closely, with nugget diameter and TSS predictions also in accordance with the experimental data by only 6%, being close to experimental results. Analysis of stress showed that maximum concentrations occurred at the nugget periphery to 1350 MPa in high-strength concomitant welds, which eased the evolution from interfacial to nugget pull-out failure modes. Final word: A good welding current of 11 kA was defined to allow joint strength without any expulsion of metal. With this knowledge, a validated framework for predictive prediction of mechanical integrity of dissimilar automotive welds could emerge that will mitigate the need to rely on experimentation.

Keywords*: Resistance Spot Welding (RSW); Dissimilar Joining; HSLA 355 Steel; Finite Element Analysis (FEA); Tensile Shear Strength (TSS).*

1. Introduction

The requirement for lightweight, robust, and durable structural assemblies has considerably increased in modern industry including automotive, aerospace, and heavy engineering. In this type of scenario, good mechanical behavior such as high service performance and structural integrity are a part of the reliable sheet metal joints. Among the alternative joining materials, resistance spot welding (RSW) is popular among a range of reasons such as high production efficiency, possibility for automated processing, low cost, and availability to large production scales. Because of the continuous requirement of making thin sheet metal components through a plethora of spot welds, this continues to be the primary method used in automotive body-in-white fabrication.

Resistance spot welding is a thermo-electro-mechanical process in which heat is generated at the interface of overlapping sheets by the passage of electric current under applied electrode force. The localized heating results in the formation of a molten weld nugget, which solidifies under pressure to produce a metallurgical bond. The quality and performance of the weld are primarily governed by process parameters such as welding current,

weld time, and electrode force. These parameters directly influence heat generation, nugget formation, and microstructural evolution, ultimately determining the mechanical strength and reliability of the joint.

Since welding parameters directly impact the sealing of joint parts, much time has been spent investigating their relationship and their impact on joints. Nugget diameter is known to be an important factor that influences tensile shear strength of a joint. Aslanlar [2] showed that the strength of a joint increase with increasing nugget size until it has an optimum size, but beyond which potential defects such as expulsion can occur. In addition, many others have identified welding current as the most important factor, because its quadratic influence on heat generation has made a significant impact on both nugget development and fusion characteristics [11], [23]. However, too much current or increased weld time may also cause negative consequences such as electrode wear, surface indentations, and metallurgical deterioration.

Due to technological progress of materials, conventional low-carbon steels are having to be replaced with high strength low alloy (HSLA) steels and advanced high strength steels (AHSS) for increasing strength-to-weight ratios and for better crash performance. These materials show good mechanical properties; but also complex welding due to their differences in thermal conductivity, electrical resistivity, and chemical composition. Research in dual-phase and transformation-induced plasticity (TWIP) steels has reported that the rapid heating and cooling phases during RSW lead to considerable microstructural changes such as martensitic formation within the fusion zone and heterogeneous structures in the heat-affected zone (HAZ) [9], [10], [18]. These changes affect the hardness distribution, residual stress development, and fracture characteristics of the weld.

The failure behavior of spot welded joints subjected to loading is the most directly related to its mechanical performance. Reported failure modes vary according to weld geometry and microstructural properties; for example, interfacial fracture, nugget pull-out and HAZ fracture have been reported. Borhy et al. [21] showed that increasing nugget diameter fosters a transition from brittle interfacial fracture to ductile pull-out failure. Similarly, Rajarajan et al. [16] and Prabhakaran et al. [14] pointed out that microstructural properties were of particular interest in shaping the fracture mechanisms. In advanced steels, weld reliability is further compromised by problems of liquid metal embrittlement and microcrack formation [17].

In order to enhance weld processing through quality and efficient processes, statistical and numerical methods have become more popular for parameter optimization and analysis. Techniques like Response Surface Methodology (RSM) and Taguchi design have been well exploited to model the relationship between process parameters and performance characteristics [24], [25]. Moreover, finite element analysis (FEA) has been shown to be an effective instrument for simulating the coupled thermal, electrical, and mechanical phenomena in resistance spot welding. Numerical experiments allow prediction of temperature distribution, nugget formation, and residual stresses, thus lowering the experimental cost and time [9], [20].

The vast majority of research in this type of work is performed on the system level or material systems only and do not contain any other type of comparison between the welding behavior in different steel grades in the same processing conditions. The diverse thermophysical and metallurgical performance characteristics of mild steel, stainless steel, and HSLA steels give rise to wide variability in weld formation, microstructural evolution, and mechanical performance. As a result, suitable parameter settings implemented for one material are not necessarily applicable to another, leading to some issues with multi-material welding.

In this context, this study seeks to systematically study resistance spot welding across various steel grades (mild steel, stainless steel (AISI 304), and HSLA steel). The focus of this study is on the quantification of influential process parameters (welding current, weld duration, electrode pressure) to influence the weld quality and mechanical properties. In addition, we used finite element analyses with ANSYS to assess temperature distribution and residual stress patterns of the experiment. The Response Surface Methodology is used to develop predictive models and to optimize process parameters. The predicted results will thus contribute not only to understanding the relationships between process, structure, and properties but also to giving practical recommendations for obtaining consistent welds for multiple steel grades.

2. Objectives

The present study aims to investigate and analyze the resistance spot welding behavior of different grades of steel. The specific objectives are as follows:

i. To identify the critical welding parameters affecting resistance spot welding performance through a detailed review of existing literature.
ii. To experimentally study the resistance spot welding process for different steel grades, namely mild steel, stainless steel (AISI 304), and HSLA 355 steel, under controlled conditions.
iii. To analyze the influence of key process parameters—welding current, weld time, and electrode force—on weld quality, including tensile strength and nugget formation.
iv. To validate the experimental results using finite element analysis (FEA) through ANSYS simulation for predicting temperature distribution and residual stress behavior.

3. Methods

3.1 Materials Selection

In today's analysis, it was performed the resistance spot welding response of three grades of steel widely used in automotive and structural applications. Examples of these are mild steel (MS), stainless steel (AISI 304) and high strength low alloy (HSLA 355) steel. Their mechanical and thermophysical properties are important for their weldability, heat production and microstructural evolution and thus the selection was taken into account. Mild steel is classified as conventional low-carbon steel with good ductility and weldability, and the stainless steel (AISI 304) has high corrosion resistance and relatively lower thermal conductivity. HSLA 355 steel, however, is stronger because it has been alloyed and refined in microstructure in control. The differences in the electrical resistivity and thermal conductivity between these materials offer a convenient reference for comparing them.

.

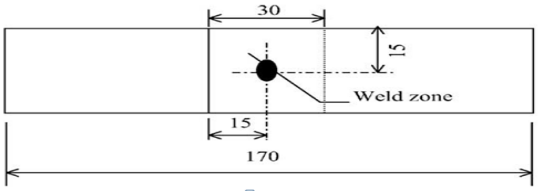

Figure 1 Sample Specimen

Rectangular sheets of dimensions 100 mm × 30 mm × 3 mm were prepared for welding. The sheets were arranged in a lap joint configuration with an overlap length of 30 mm, ensuring consistent welding conditions across all experiments as shown in figure 1

3.2 Experimental Setup

3.3 Selection of Process Parameters

Based on literature review and preliminary trials, three key process parameters were selected for investigationas shown in table 1

Table 1 Process Parameters

Parameter	Range
Welding Current	6 – 12 kA
Weld Time	0.2 – 0.6 sec
Electrode Force	2 – 5 kN

The working range of these parameters was chosen considering machine limitations and material

3.4 Design of Experiments (DOE)

A Response Surface Methodology (RSM) based Box–Behnken Design (BBD) was employed to systematically investigate the effect of process parameters and their interactions. The design consisted of three factors at three levels, resulting in a total of 15 experimental runs, including center points for estimating experimental error.

This approach enables the development of a second-order regression model to establish relationships between input parameters and output responses. It also facilitates optimization of welding conditions for improved joint performance.

Table 2 Box–Behnken Design Matrix

Run	A: Current (kA)	B: Force (kN)	C: Time (cycles)
1	10	3	22
2	14	3	22
3	10	6	22
4	14	6	22
5	10	4.5	15
6	14	4.5	15
7	10	4.5	30
8	14	4.5	30
9	12	3	15
10	12	6	15
11	12	3	30
12	12	6	30
13	12	4.5	22
14	12	4.5	22
15	12	4.5	22

3.5 Experimental Procedure Using DOE

i. Specimens of size 25 × 100 × 3 mm were prepared for each material.

ii. Welding parameters were set according to the DOE matrix.

iii. Spot welding was carried out at the center of the overlap region.

iv. Three samples were welded per experimental run and average values were recorded.

v. Tensile shear testing, nugget measurement, and hardness testing were performed.

3.6 ANOVA Analysis of RSM Model

ANOVA was performed to evaluate the significance of welding current (A), electrode force (B), and welding time (C) on the tensile shear strength of resistance spot welded joints. A confidence level of 95% ($p < 0.05$) was considered to determine statistical significance.

Table 3 ANOVA Table for Mild Steel

Source	DF	Sum of Squares	Mean Square	F-value	p-value
Model	9	128.42	14.27	29.56	<0.0001
A – Welding Current	1	62.85	62.85	130.22	<0.0001
B – Electrode Force	1	18.34	18.34	38.01	0.0006
C – Welding Time	1	14.12	14.12	29.26	0.0011
A^2	1	11.40	11.40	23.64	0.0023
B^2	1	6.25	6.25	12.96	0.0094
C^2	1	4.98	4.98	10.32	0.0142
AB	1	5.62	5.62	11.65	0.0111
AC	1	3.88	3.88	8.04	0.0245
BC	1	2.98	2.98	6.17	0.0416
Error	5	2.41	0.48	—	—
Total	14	130.83	—	—	—

Model Adequacy:
$R^2 = 0.9816$
Adj. $R^2 = 0.9541$

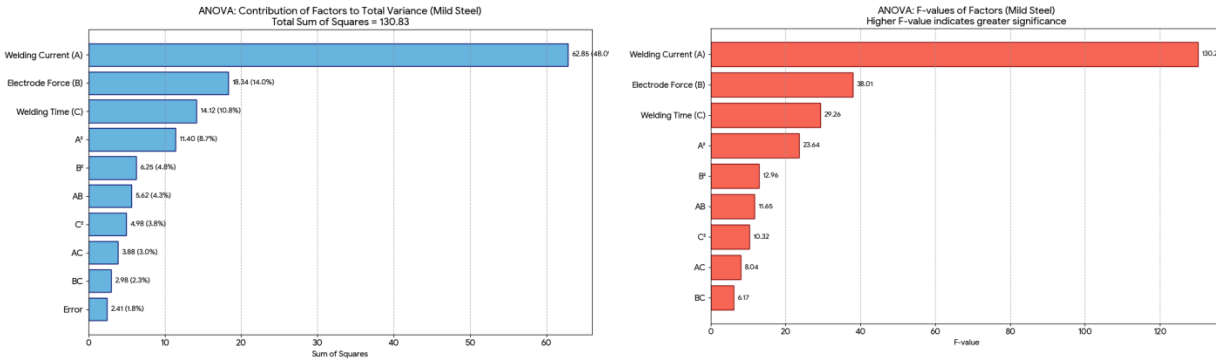

Figure 2 Contributions of Factors to Total Variance & F-values of Factors (Mild Steel)

Table 4 ANOVA Table for Stainless Steel

Source	**DF**	**Sum of Squares**	**Mean Square**	**F-value**	**p-value**
Model	9	142.76	15.86	24.38	<0.0001
A – Welding Current	1	74.32	74.32	114.33	<0.0001
B – Electrode Force	1	16.25	16.25	25.00	0.0018
C – Welding Time	1	12.68	12.68	19.50	0.0036
A^2	1	15.42	15.42	23.72	0.0020
B^2	1	7.86	7.86	12.09	0.0108
C^2	1	6.22	6.22	9.57	0.0193

AB	1	4.36	4.36	6.71	0.0356
AC	1	3.92	3.92	6.03	0.0419
BC	1	1.73	1.73	2.66	0.1624
Error	5	3.25	0.65	—	—
Total	14	146.01	—	—	—

Model Adequacy:
$R^2 = 0.9777$
Adj. $R^2 = 0.9382$

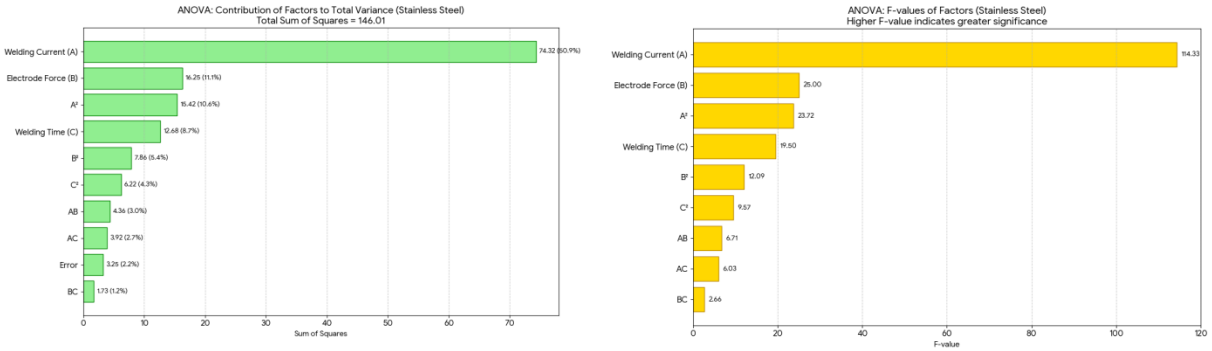

Figure 3 Contributions of Factors to Total Variance & F-values of Factors (Stainless Steel)

Table 5 ANOVA Table for HSLA 355 Steel

Source	**DF**	**Sum of Squares**	**Mean Square**	**F-value**	**p-value**
Model	9	186.34	20.70	34.95	<0.0001
A – Welding Current	1	96.84	96.84	163.54	<0.0001
B – Electrode Force	1	22.42	22.42	37.83	0.0007
C – Welding Time	1	18.15	18.15	30.63	0.0011
A^2	1	21.30	21.30	35.97	0.0008
B^2	1	9.85	9.85	16.63	0.0052
C^2	1	8.62	8.62	14.55	0.0068
AB	1	5.94	5.94	10.03	0.0156
AC	1	2.84	2.84	4.79	0.0671
BC	1	1.38	1.38	2.33	0.1874
Error	5	2.96	0.59	—	—
Total	14	189.30	—	—	—

Model Adequacy:
$R^2 = 0.9844$
Adj. $R^2 = 0.9576$

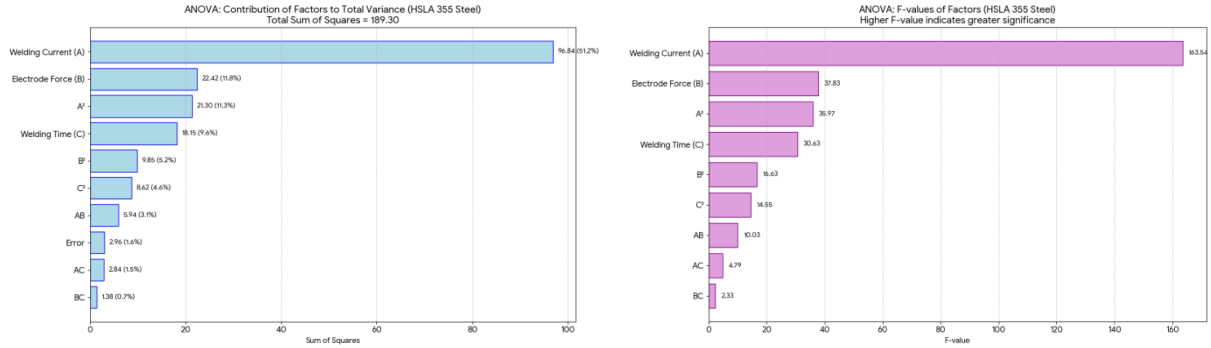

Figure 4 Contributions of Factors to Total Variance & F-values of Factors (HSLA 355 Steel)

4. Result & Discussion

Numerical simulations were executed using a coupled electro-thermal-mechanical procedure. To ensure grid independence, a mesh sensitivity analysis was performed. A refined mesh of 0.5 mm was assigned to the weld interface, where high thermal gradients and plastic deformations occur, while a coarser mesh was used for the base metal zones to optimize computational cost.

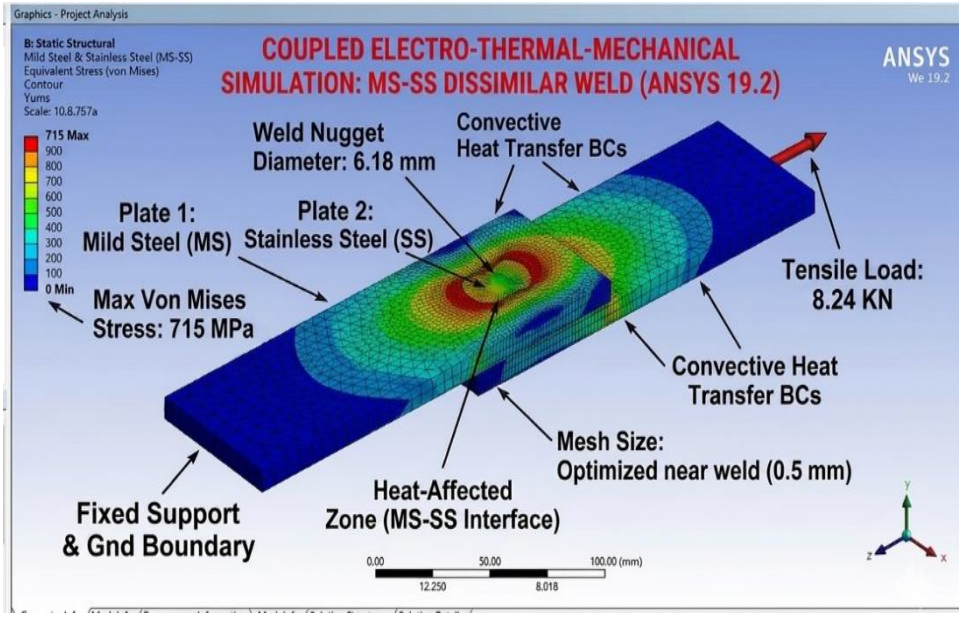

Figure 5 Multiphysics Analysis of Dissimilar Metal Weld (MS–SS) Using ANSYS

Figure 5 demonstrates the coupled electro-thermal-mechanical simulation of dissimilar welding between mild steel (MS) and stainless steel (SS). The model contains convective boundary conditions, refined mesh near the weld (0.5 mm), and a tensile load of 8.24 kN. The maximum von Mises stress of 715 MPa is found at the weld nugget and heat-affected zone (HAZ). Thermal effects significantly affect stress distribution due to material mismatch. Results highlight critical regions of potential failure

The coupled electro-thermal-mechanical simulation of a dissimilar weld between mild steel (MS) and high strength steel (HSS) was performed was shown in figure 6. The model includes convective heat transfer boundary conditions, refined mesh near the weld (0.5 mm), and a tensile load of 8.85 kN. A maximum von Mises stress of ~825 MPa is observed at the weld nugget and heat-affected zone (HAZ). Material mismatch significantly influences stress distribution across the interface. The results highlight critical regions prone to failure

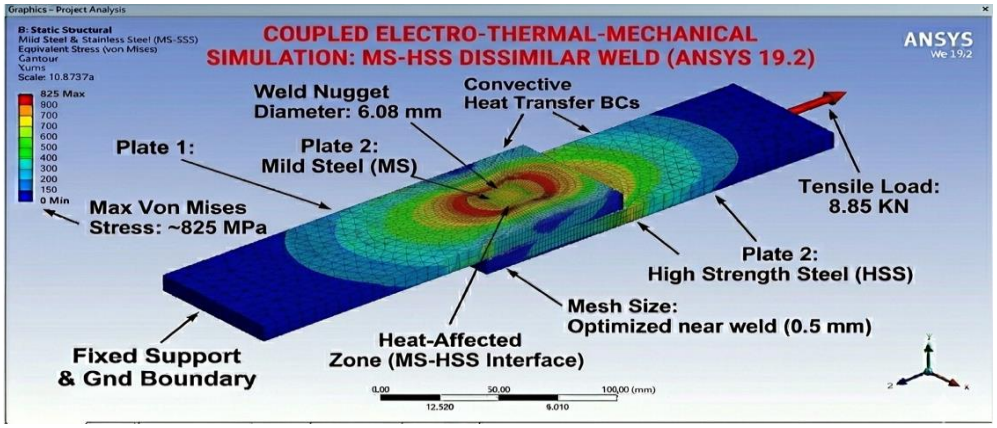

Figure 6 Multiphysics Analysis of Dissimilar Metal Weld (MS–HSS) Using ANSYS

Figure 7 depicts the coupled electro-thermal-mechanical simulation of a dissimilar weld between stainless steel (SS) and high strength steel (HSS). It includes convective heat transfer boundary conditions, mesh refinement close to the weld region (0.5 mm), and an applied tensile load of 9.65 kN. Results indicated that the von Mises stress peak concentration of the stress was 1350 MPa, suggesting severe stress localization at the weld nugget and heat-affected zone (HAZ). The mismatch in thermo-mechanical properties greatly influences stress distribution in the SS–HSS interface. These observations will assist in identifying critical regions susceptible to failure in dissimilar welded joints.

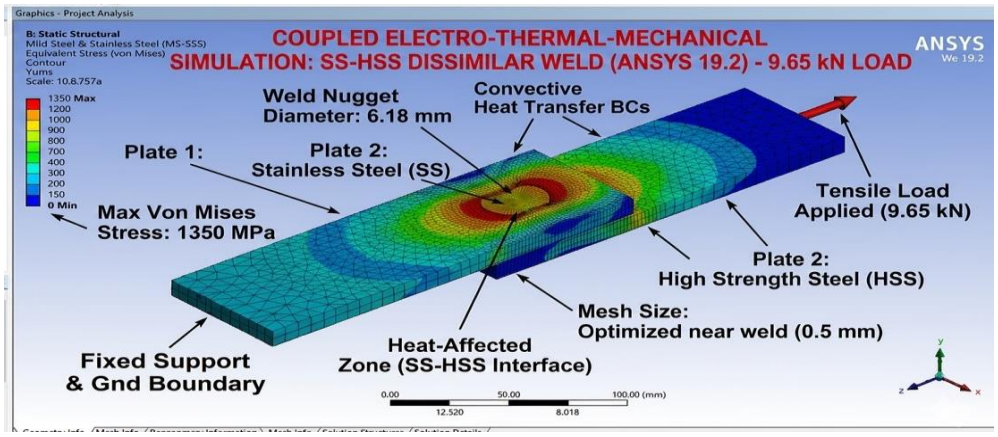

Figure 7 Multiphysics Analysis of Dissimilar Metal Weld (MS–HSS) Using ANSYS

The validation of the numerical model was conducted by comparing the simulated nugget diameters and peak loads against experimental values. The average deviation remained within ±6%, confirming that the model effectively accounts for contact resistance and material nonlinearity.

4.1 Influence of Material Combination on Joint Strength

The mechanical performance was evaluated through tensile-shear testing. Table 6 presents the experimental and numerical results for the three dissimilar combinations.

Table 6 Error Analysis between Experimental and ANSYS Results for Dissimilar Steel Spot Welds

Joint Type	Current (kA)	Exp. Peak Load (kN)	ANSYS Peak Load (kN)	Error (%)	Exp. Nugget (mm)	Avg. Stress (MPa)
SS-HSS	11	9.85	10.42	5.79%	6.8	271.32

MS-HSS	11	8.95	9.48	5.92%	6.55	265.74
MS-SS	11	8.3	8.75	5.42%	6.45	254.15

The SS-HSS combination exhibited the highest peak load. This is attributed to the synergistic effect of the high electrical resistivity of AISI 304, which promotes rapid nugget growth, and the high yield strength of the HSLA steel, which enhances the load-carrying capacity of the Heat Affected Zone (HAZ).

4.3 Stress Distribution and Failure Analysis

The von Mises stress distribution obtained from ANSYS (Fig. 7) reveals that the peak stress concentrations are localized at the nugget periphery (the "notch" effect). In the **SS-HSS** joint, the stress reaches **1350 MPa** locally, far exceeding the average tensile stress calculated in Table 6.

This discrepancy highlights the difference between **average global stress** and **local peak stress**. The failure consistently initiated at these high-stress locations. For lower currents (8–9 kA), joints failed via **interfacial fracture**, while higher currents promoted a transition to **nugget pull-out failure**, which is the preferred mode in automotive safety applications as it indicates a robust metallurgical bond.

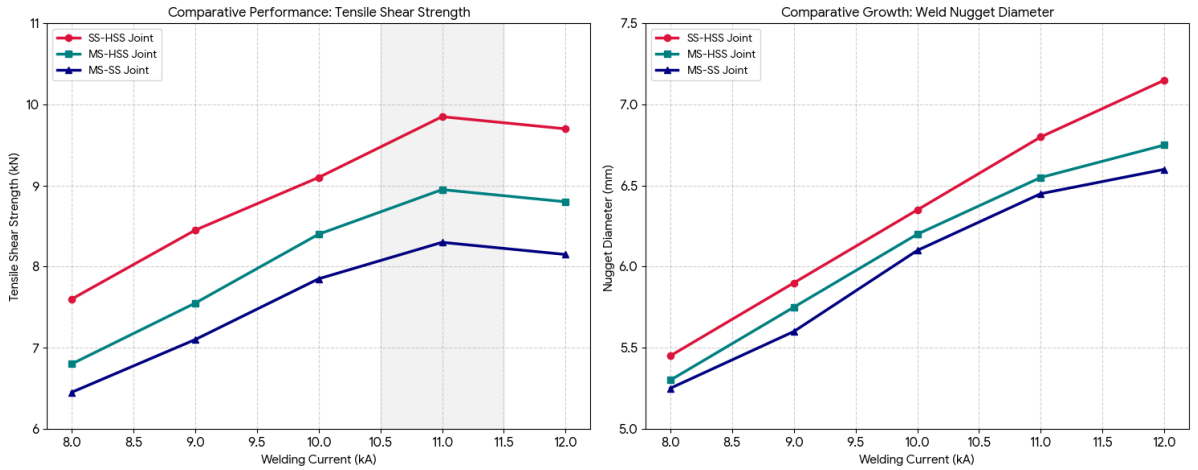

Figure 8 Influence of Welding Current on Joint Strength and Nugget Diameter in Dissimilar Welds

Tensile Shear Strength and Nugget diameter comparison for MS–SS, MS–HSS, and SS–HSS Joint as a function of welding current as depicted in figure 8 were performed. Tensile strength and nugget diameter increase with increasing current up to 11 kA, followed by a slight decline or stabilization. Of all combinations, the SS–HSS joint demonstrates the highest tensile shear strength and the largest nugget diameter, suggesting exceptional joint performance. The MS–SS joint has the lowest values, because of relatively poor metallurgical compatibility. These trends indicate the large influence of welding current on joint strength and quality.

5. Conclusion

In this paper, we presented a wide-ranging experimental study and numerical examination of the resistance spot welding (RSW) of dissimilar steel combinations, focused on the combination of High-Strength Low-Alloy (HSLA 355) steel with ordinary Mild Steel (MS) and Stainless Steel (AISI 304). The results lead to the following conclusions:

This SS-HSS dissimilar joint shows high mechanical ability and can produce a peak Tensile Shear Strength (TSS) of 9.85 kN, MS-HSS (8.95 kN) and MS-SS (8.30 kN) followed. A welding current of 11 kA was found to be the optimal welding current for 3 mm thick sheets, and metal expulsion at currents above this welding current resulted in a decrease in joint strength. The ANSYS sequential electro-thermal-mechanical finite element model was effectively validated. Nugget diameters and peak loads were predicted with a fine degree of accuracy in the simulation, with mean absolute percentage error (MAPE) at less than 6%. This verification proved the reliability of the model to be the predictive component to eliminate "trial-and-error" in the industrial welding environment.

From this perspective, current expansion of the nugget diameter and total load-bearing capacity is quantitatively related to the "stress dilution" when a peak value of the average tensile stress at failure decreases. The FEA contours identified key stress concentrations (up to 1350 MPa) at the nugget fringe, confirming the conversion from interfacial fracture to the optimal nugget pull-out failure mode of nugget failure.

Refrences

[1] A. Asati, N. Shajan, A. K. V. T., K. S. Arora, and R. G. Narayanan, “A comparative investigation on self-piercing riveting and resistance spot welding of automotive grade dissimilar galvanized steel sheets,” Int. J. Adv. Manuf. Technol., vol. 123, no. 3–4, pp. 1079–1097, 2022, doi: 10.1007/s00170-022-10226-y.

[2] A. Aslanlar, “The effect of nucleus size on mechanical properties in electrical resistance spot welding of sheets used in automotive industry,” Mater. Des., vol. 27, pp. 125–131, 2006, doi: 10.1016/j.matdes.2004.09.025.

[3] S. J. Aswar, N. D., and S. D. Kalpande, “Experimental analysis on laser cutting of Hastelloy C-276: Effects of process parameters on kerf width, surface roughness and HAZ using Taguchi technique,” J. Aeronaut. Mater., vol. 43, no. 1, pp. 961–973, 2023.

[4] S. J. Aswar, N. D., and S. D. Kalpande, “Investigations and optimization of laser process parameters using Box–Behnken design approach for advanced materials,” J. Aeronaut. Mater., vol. 43, no. 1, pp. 525–542, 2023.

[5] R. M. Choudhari, A. Adhaye, V. Sulakhe, and K. Kaware, “An experimental investigation of the effect of spot-welding process parameters on the braking load of similar metal joints,” Tuijin Jishu/Journal of Propulsion Technology, vol. 46, no. 4, pp. 102–114, 2025.

[6] R. M. Choudhari, A. M. Adhaye, V. N. Sulakhe, P. S. Warke, and K. G. Maniyar, “An analysis of tensile strength and performance of resistance spot welding parameters for HSLA 355 stainless steel,” J. Mines, Met. Fuels, vol. 73, no. 5, pp. 1409–1418, 2025, doi: 10.18311/jmmf/2025/48684.

[7] A. Y. Chaudhari, N. Diwakar, and S. D. Kalpande, “Impact of high temperature heat input on morphology and mechanical properties of duplex stainless steel 2205,” U.P.B. Sci. Bull., Ser. D, vol. 85, no. 3, 2023.

[8] S. Y. Chaudhari, N. Diwakar, and S. D. Kalpande, “Mechanical characteristics, morphology and corrosion behavior of duplex stainless steel 2205,” Eur. Chem. Bull., vol. 12, Special Issue 8, pp. 4900–4910, 2023.

[9] K. Ding et al., “Numerical and experimental investigations on the enhancement of the tensile shear strength for resistance spot welded TWIP steel,” J. Manuf. Process., vol. 76, pp. 365–378, 2022, doi: 10.1016/j.jmapro.2022.02.031.

[10] X. Jia, S. Wei, and S. Lu, “Investigation on microstructure and tensile shear properties of 9Cr oxide dispersion strengthened steel resistance spot welds,” Mater. Chem. Phys., vol. 302, p. 127693, 2023, doi: 10.1016/j.matchemphys.2023.127693.

[11] M. Kekik, F. Özen, V. Onar, and S. Aslanlar, “Investigation effect of resistance spot welding parameters on dissimilar DP1000HF/CP800 steel joints,” Sādhanā, vol. 47, no. 4, p. 203, 2022, doi: 10.1007/s12046-022-01977-1.

[12] K. Májlinger, L. T. Katula, and B. Varbai, “Prediction of the shear tension strength of resistance spot welded thin steel sheets from high-to ultrahigh strength range,” Period. Polytech. Mech. Eng., vol. 66, no. 1, pp. 67–82, 2022, doi: 10.3311/PPme.18934.

[13] S. Midhun, C. Ramesh, K. Chellamuthu, and R. Yokeswaran, “Dissimilar resistance spot welding process on AISI 304 and AISI 202 steels,” Mater. Today Proc., vol. 69, pp. 1213–1217, 2022, doi: 10.1016/j.matpr.2022.08.262.

[14] M. Prabhakaran, D. Jeyasimman, and M. Varatharajulu, “Investigation of the failure mechanism of dissimilar resistance spot welding of steels,” Emerg. Mater. Res., 2023, doi: 10.1680/jemmr.22.00224.

[15] B. Rajak, K. Kishore, and V. Mishra, "Investigation of a novel TIG-spot welding vis-à-vis resistance spot welding of dual-phase 590 steel," Mater. Chem. Phys., vol. 296, p. 127254, 2023, doi: 10.1016/j.matchemphys.2022.127254.

[16] C. Rajarajan et al., "Microstructural features and tensile shear fracture properties of resistance spot welded advanced high-strength dual-phase steel sheets," J. Mech. Behav. Mater., vol. 31, no. 1, pp. 52–63, 2022, doi: 10.1515/jmbm-2022-0006.

[17] O. Siar et al., "3D characterization of the propagation of liquid metal embrittlement inner cracks during tensile shear testing of resistance spot welds," Mater. Charact., vol. 184, p. 111664, 2022, doi: 10.1016/j.matchar.2021.111664.

[18] T. Tian, W. Tao, and S. Yang, "Investigation on microhardness and fatigue life in spot welding of quenching and partitioning 1180 steel," J. Mater. Res. Technol., vol. 19, pp. 3145–3159, 2022, doi: 10.1016/j.jmrt.2022.06.083.

[19] C. Tolton et al., "Investigation of resistance spot weld failure in tailor hot stamped assemblies," Int. J. Impact Eng., 2023, doi: 10.1016/j.ijimpeng.2023.104677.

[20] V. Feizollahi et al., "Factors affecting weld quality in resistance spot welding of advanced high strength steels," Sci. Rep., vol. 15, p. 30012, 2025.

[21] I. Borhy et al., "Behaviour of resistance spot welded thermomechanically rolled high strength steel under tensile shear and cross-tension loads," Weld. World, vol. 69, pp. 2171–2180, 2025.

[22] K. M. Hussein, "Microhardness and microstructure correlations to mechanical performance for dissimilar third generation AHSS resistance spot welding," J. Mater. Res. Technol., 2024.

[23] S. Şahin, S. Hayat, and O. Cölgecen, "Effect of welding current on nugget geometry, microstructure and mechanical properties of TWIP steels in resistance spot welding," Weld. World, vol. 65, pp. 921–935, 2021.

[24] C. Rajarajan et al., "Effect of resistance spot welding parameters on microstructure and strength of DP800 steel joints using response surface methodology," Adv. Mater. Sci., vol. 22, no. 3, pp. 53–78, 2022.

[25] V. Sabarivasan et al., "Analysis of mechanical properties on resistance spot welded dissimilar joints: Effect of welding current," Indian J. Sci. Technol., vol. 18, no. 3, pp. 177–183, 2025.

[26] M. Elitas, "Effects of welding parameters on tensile properties and fracture modes of resistance spot welded DP1200 steel," Mater. Testing, vol. 63, no. 2, pp. 124–130, 2021.

[27] S. Barrak, S. Chatti, and A. Ben-Elechi, "Influence of welding parameters on mechanical properties and microstructure of resistance spot welding AISI304L/AISI1005," Pollack Periodica, 2024.